Storage and retrieval of interacting photons in a Rydberg medium

Liu Yang,[1] Bing He,[2,*] and Min Xiao[3]

[1]*College of Automation, Harbin Engineering University, Harbin 150001, China*
[2]*Center for Quantum Optics and Quantum Information, Universidad Mayor, Camino La Pirámide 5750, Huechuraba, Chile*
[3]*Department of Physics, University of Arkansas, Fayetteville, Arkansas 72701, USA*

Storing interacting photons in ensembles of highly excited Rydberg atoms makes it possible to realize photon-photon gates. The efficiency of stopping and retrieving pairs of single-photon pulses in any Rydberg medium is, however, significantly influenced by their mutual interaction. The corresponding dynamical process is rather complicated due to the interaction constantly changing with the relative positions of photon pulses and the associated dissipation. Applying the numerical calculations based on first principles, we reveal the detail of such a dynamical process by showing how the interacting pulses evolve in various situations. Other important issues, such as the use of nonadiabatic passage for stopping photons and the optimal way to regenerate photons, are also investigated.

I. INTRODUCTION

Photons are ideal carriers of quantum information as they travel fast and interact weakly with the environment. However, a sufficient magnitude of interaction between photons will be necessary if one needs to use them directly for information processing. Photon-photon interactions realized by various nonlinear optical mechanisms are thus essential to quantum information processing [1–4]. Mapping the strong interactions between Rydberg atoms onto those between single photons via electromagnetically induced transparency (EIT) has emerged as a promising approach for the purpose. The possible applications of the mechanism include photonic logic gates [5–7], single photon generation [8], creation of entanglement between light and atomic excitations [9], all-optical switches and transistors [10–13], single-photon absorbers [14], and others [15–18]. Some effects related to photon-photon interaction have been experimentally observed in a cold Rydberg EIT medium [19,20].

In addition to strong interatomic interaction, Rydberg atoms have long lifetimes scaling as the power law n^3 with the principal quantum number n of the energy levels. It is advantageous to the storage of photons in an ensemble of Rydberg atoms. As one of the important applications, photonic gate operation generally proposed with photons slowed down in an EIT medium [5,6,21] can be even performed with the stopped photons converted to Rydberg atomic excitations [22,23], which achieve a much higher phase shift for a controlled phase (CP) gate operation than the cross-phase modulation (XPM) by ordinary Kerr nonlinearity [24,25]. Recently some experiments [26–28] have demonstrated strong XPM between weak light pulses, and one of them based on Rydberg atomic ensemble reported the realization of a π-radian phase shift [26]. On the other hand, the storage and retrieval of optical

photons in EIT media of cold [16,29,30] or thermal [31] Rydberg atoms were experimentally investigated too. However, because the interaction between photons brings about some unwanted effects such as the extra dissipation due to breaking the EIT condition under interaction, it was not fully clear how such a process of storing and retrieving photons can be well performed in reality. To understand such processes of individually prepared but mutually interacting photons, it is also necessary to have a dynamical picture appropriate to the unfixed interaction between photon pulses instead of the steady state picture (see, e.g., [19]) widely adopted in the past.

So far the storage and retrieval of a multiphoton pulse in Rydberg EIT media has been theoretically studied to understand how the pulse with multiple photons is stopped and regenerated under its self-interaction [32]. The used approach is based on the superatom (SA) model [33] that was proposed to explain the propagation of a multiphoton beam in a Rydberg EIT medium [34]. According to the model, the response of the medium (such as its atomic polarization function) to the pulse of many photons is the superposition of two parts; one is that of two-level atomic structure due to the Rydberg blockade formed within the pulse, and the other is that of a three-level system from the remnant EIT effect. To a pulse containing only one single photon, however, no Rydberg blockade occurs within the pulse itself because its exciting a single Rydberg atom cannot be blocked unless the atom is under the strong interaction with other atoms. In other words, Rydberg blockade happens only when the pulse is within the blockade radius of Rydberg excitations induced by other pulses getting very close to it. The model of SA is therefore not applicable to the processes involving a number of such single-photon pulses.

In this paper we apply a dynamical approach detailed in Sec. II to study the evolutions of two interacting photon pulses during their storage and retrieval in a cold Rydberg atomic medium, which are beyond the applicability of the SA model. We analyze how single-photon pulses are converted to stationary spinwave under their mutual interaction in a Rydberg

*bing.he@umayor.cl

043827-1
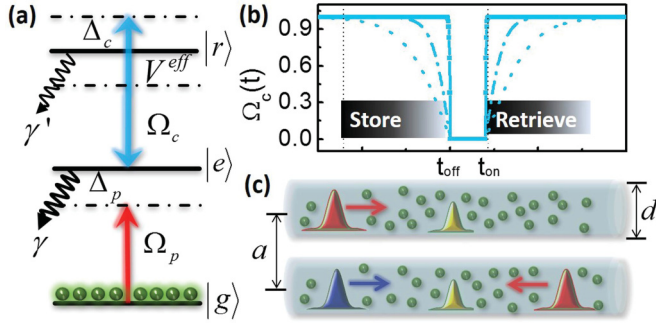
FIG. 1. (a) Energy-level scheme of a Ξ-type or ladder-type atomic system. Here $\Delta_p = \omega_{eg} - \omega_p$ and $\Delta_c = \omega_{re} - \omega_c$, as the differences between a level gap and a field central frequency. (b) Coupling field $\Omega_c(t) = \Omega_c^M \tanh\{(t_{\text{off}} - t)/\tau_{\text{off}}\}$ $(t \leqslant t_{\text{off}})$; $\Omega_c(t) = 0$ $(t_{\text{off}} < t < t_{\text{on}})$; $\Omega_c(t) = \Omega_c^M \tanh\{(t_{\text{on}} - t)/\tau_{\text{on}}\}$ $(t \geqslant t_{\text{on}})$ switched off at t_{off} and on at t_{on} for realizing the storage and retrieval of a photon pulse. The solid, dot-dashed, and dotted curves indicate those with the gradually slowing speed of switch (corresponding to the increasing τ_{off} and τ_{on}). (c) Geometry of the pulse propagations. The diameter of each ensemble is d and the distance between the axes of the two ensembles is a. Two single-photon pulses propagate in two different ensembles either along the same direction like the red and blue one or from the opposite tips like the two red ones. The pulses are stopped in the ensembles as the yellow ones with their amplitudes diminished from the damping in the medium, and interact with each other through the long-range van der Waals potential.

medium in Sec. III. In the same section we also discuss the effects of fast/slow switch (nonadiabatic passage/adiabatic passage) of control fields on the transfer between propagating photons and Rydberg spinwaves, as well as the optimal strategy to retrieve the stopped photons under mutual interaction. The main purpose of the research is to provide a quantitative picture for quantum information processing with photons in a Rydberg atomic media.

II. THEORETICAL APPROACH

In Fig. 1 we illustrate a setup for stopping and regenerating interacting photons in two different pencil shaped ensembles. Here two single-photon pulses can either travel along the same direction (copropagation) or respectively come from the opposite tips (counterpropagation). The pulses are separated into two ensembles to avoid Rydberg blockade. The control fields with the Rabi frequency $\Omega_c(t)$ are being turned off with time so that the pulses will be stopped at two nearby locations inside the ensembles. After the two converted spinwave packets interact via long-range interaction potential for a certain time, the control fields will be turned on again to retrieve the propagating pulses. Similar processes can also be implemented with properly arranged pulses in a single ensemble [6].

The propagation of the photons can be described by the kinetic Hamiltonian ($\hbar = 1$)

$$H_p = -ic \int d\mathbf{x} \hat{\mathcal{E}}_1^\dagger(\mathbf{x}) \partial_z \hat{\mathcal{E}}_1(\mathbf{x}) \mp ic \int d\mathbf{x} \hat{\mathcal{E}}_2^\dagger(\mathbf{x}) \partial_z \hat{\mathcal{E}}_2(\mathbf{x}) \quad (1)$$

of the electromagnetic field $\hat{\mathcal{E}}_l(\mathbf{x}, t)$ $(l = 1, 2)$, where "$-$" before the second term corresponds to copropagating and "$+$" to counterpropagating. The level scheme in Fig. 1(a) involves the induced atomic polarization field $\hat{P}_l(\mathbf{x}, t) = \sqrt{N} \hat{\sigma}_{ge}^l(\mathbf{x}, t)$ and spinwave field $\hat{S}_l(\mathbf{x}, t) = \sqrt{N} \hat{\sigma}_{gr}^l(\mathbf{x}, t)$. The operator $\hat{\sigma}_{\mu\nu} = |\mu\rangle\langle\nu|$ distributing over a high-density ensemble can be treated as a continuous field. The high atomic density N enhances the atom-field coupling (with the constant g) as seen in the Hamiltonian

$$H_{af} = -\sum_{l=1}^{2} \int d\mathbf{x} \{ g\sqrt{N} \hat{\mathcal{E}}_l^\dagger(\mathbf{x}) \hat{P}_l(\mathbf{x}) + \Omega_c(t) \hat{S}_l^\dagger(\mathbf{x}) \hat{P}_l(\mathbf{x}) + \text{H.c.} \}$$

$$+ \sum_{l=1}^{2} \int d\mathbf{x} \Delta_p \hat{P}_l^\dagger(\mathbf{x}) \hat{P}_l(\mathbf{x}), \quad (2)$$

about the atomic level scheme in Fig. 1(a) (a similar Hamiltonians for a Λ-type system is given in, e.g., [35]). This Hamiltonian indicates that the input photons cause the transition between $|g\rangle$ and $|e\rangle$ with the coupling constant $g\sqrt{N}$, while the control fields render the transition between $|e\rangle$ and $|r\rangle$ at the coupling Rabi frequency $\Omega_c(t)$. A narrow-band pulse propagates with negligible absorption under the EIT condition $\Delta_p + \Delta_c = 0$. However, under the interaction of the spinwave fields described by

$$H_{\text{int}} = \int d\mathbf{x} \int d\mathbf{x}' \hat{S}_1^\dagger(\mathbf{x}) \hat{S}_2^\dagger(\mathbf{x}') \Delta(\mathbf{x} - \mathbf{x}') \hat{S}_2(\mathbf{x}') \hat{S}_1(\mathbf{x}), \quad (3)$$

where

$$\Delta(\mathbf{x} - \mathbf{x}') = C_6/|\mathbf{x} - \mathbf{x}'|^6$$

is the van der Waals potential, the EIT condition will be violated by shifting the level $|r\rangle$ of the relevant Rydberg atoms. The consequent dissipation from populating the levels that decay at the rates γ and γ' can be depicted by a stochastic Hamiltonian

$$H_{\text{dis}} = i\sqrt{2\gamma} \sum_{l=1}^{2} \int d\mathbf{x} \{ \hat{\zeta}_l^\dagger(\mathbf{x}, t) \hat{P}_l(\mathbf{x}) - \hat{\zeta}_l(\mathbf{x}, t) \hat{P}_l^\dagger(\mathbf{x}) \}$$

$$+ i\sqrt{2\gamma'} \sum_{l=1}^{2} \int d\mathbf{x} \{ \hat{\eta}_l^\dagger(\mathbf{x}, t) \hat{S}_l(\mathbf{x}) - \hat{\eta}_l(\mathbf{x}, t) \hat{S}_l^\dagger(\mathbf{x}) \}$$

$$(4)$$

involving the quantum noise fields $\hat{\zeta}_l(\mathbf{x}, t)$ and $\hat{\eta}_l(\mathbf{x}, t)$. The total Hamiltonian $H = H_p + H_{af} + H_{\text{int}} + H_{\text{dis}}$ leads to the following dynamical equations for the quantum fields:

$$\partial_t \hat{\mathcal{E}}_l(\mathbf{x}, t) + c\partial_z \hat{\mathcal{E}}_l(\mathbf{x}, t) = ig\sqrt{N} \hat{P}_l(\mathbf{x}, t), \quad (5)$$

$$\partial_t \hat{P}_l(\mathbf{x}, t) = -(\gamma + i\Delta_p) \hat{P}_l(\mathbf{x}, t) + i\Omega_c^*(t) \hat{S}_l(\mathbf{x}, t)$$

$$+ ig\sqrt{N} \hat{\mathcal{E}}_l(\mathbf{x}, t) - \sqrt{2\gamma} \hat{\zeta}_l(\mathbf{x}, t), \quad (6)$$

$$\partial_t \hat{S}_l(\mathbf{x}, t) = -\gamma' \hat{S}_l(\mathbf{x}, t) + i\Omega_c(t) \hat{P}_l(\mathbf{x}, t)$$

$$- i \int d\mathbf{x}' \Delta(\mathbf{x} - \mathbf{x}') \hat{S}_{3-l}^\dagger(\mathbf{x}', t) \hat{S}_{3-l}(\mathbf{x}', t) \hat{S}_l(\mathbf{x}, t)$$

$$- \sqrt{2\gamma'} \hat{\eta}_l(\mathbf{x}, t). \quad (7)$$

The derivation of the above equations directly with the stochastic Hamiltonian H_{dis} in Eq. (4) follows a procedure generalized from the one in, e.g., Ref. [36].

One can translate the above dynamical equations of the quantum fields into those of the two-particle functions $OO(\mathbf{x}, \mathbf{x}', t) = \langle 0, 0|\hat{O}_1(\mathbf{x}, t)\hat{O}_2(\mathbf{x}', t)|1, 1\rangle$ for the quantum fields $\hat{O}_l(\mathbf{x}, t) = \hat{\mathcal{E}}_l(\mathbf{x}, t), \hat{P}_l(\mathbf{x}, t)$, and $\hat{S}_l(\mathbf{x}, t)$ $(l = 1, 2)$ as in [19]. Here, to simplify the calculations, we adopt a different approach about the evolutions of the quantum field profiles defined as $O_1(\mathbf{x}, t) = \langle 0, 1|\hat{O}_1(\mathbf{x}, t)|1, 1\rangle$, $O_2(\mathbf{x}, t) = \langle 1, 0|\hat{O}_2(\mathbf{x}, t)|1, 1\rangle$ [37], where

$$|1\rangle = \int_{-\infty}^{\infty} d\omega f(\omega)\hat{a}^\dagger(\omega)|0\rangle \tag{8}$$

is the initial single-photon state with its frequency distribution $f(\omega)$ satisfying $\int_{-\infty}^{\infty} d\omega |f(\omega)|^2 = 1$. Multiplying $\langle 1, 0|$ or $\langle 0, 1|$ on the left of each term in Eqs. (5)–(7) and $|1, 1\rangle$ on the right side of each term in these equations, one will find the following equations for these field profiles:

$$\partial_t \mathcal{E}_l(\mathbf{x}, t) + c\partial_z \mathcal{E}_l(\mathbf{x}, t) = ig\sqrt{N}P_l(\mathbf{x}, t), \tag{9}$$

$$\partial_t P_l(\mathbf{x}, t) = -(\gamma + i\Delta_p)P_l(\mathbf{x}, t) + i\Omega_c^*(t)S_l(\mathbf{x}, t)$$
$$+ ig\sqrt{N}\mathcal{E}_l(\mathbf{x}, t), \tag{10}$$

$$\partial_t S_l(\mathbf{x}, t) = -[\gamma' + iV_l^{\text{eff}}(\mathbf{x}, t)]S_l(\mathbf{x}, t) + i\Omega_c(t)P_l(\mathbf{x}, t), \tag{11}$$

with the effective potential

$$V_l^{\text{eff}}(\mathbf{x}, t) = \frac{\int d\mathbf{x}'\{S_{3-l}^0(\mathbf{x}', t)\}^*\Delta(\mathbf{x} - \mathbf{x}')SS(\mathbf{x}, \mathbf{x}', t)}{\int d\mathbf{x}'S_{3-l}^0(\mathbf{x}', t)\}^*SS(\mathbf{x}, \mathbf{x}', t)}$$
$$\approx \frac{\int d\mathbf{x}'\Delta(\mathbf{x} - \mathbf{x}')\{S_{3-l}^0(\mathbf{x}', t)\}^*S_{3-l}(\mathbf{x}', t)}{\int d\mathbf{x}'\{S_{3-l}^0(\mathbf{x}', t)\}^*S_{3-l}(\mathbf{x}', t)}, \tag{12}$$

for $l = 1$ and 2. Here we have used an approximation $SS(\mathbf{x}, \mathbf{x}', t) \approx S_l^0(\mathbf{x})S_{3-l}(\mathbf{x}')$ [37] for narrow-band and slowly propagating pulses that are appropriate to EIT media. The spinwave profiles $S_1^0(\mathbf{x}, t) = \langle 0, 0|\hat{S}_1(\mathbf{x}, t)|1, 0\rangle$ and $S_2^0(\mathbf{x}, t) = \langle 0, 0|\hat{S}_2(\mathbf{x}, t)|0, 1\rangle$ in Eq. (12) are found with a set of exact equations in the absence of pulse interaction, i.e.,

$$\partial_t \mathcal{E}_l^0(\mathbf{x}, t) + c\partial_z \mathcal{E}_l^0(\mathbf{x}, t) = ig\sqrt{N}P_l^0(\mathbf{x}, t), \tag{13}$$

$$\partial_t P_l^0(\mathbf{x}, t) = -(\gamma + i\Delta_p)P_l^0(\mathbf{x}, t) + i\Omega_c^*(t)S_l^0(\mathbf{x}, t)$$
$$+ ig\sqrt{N}\mathcal{E}_l^0(\mathbf{x}, t), \tag{14}$$

$$\partial_t S_l^0(\mathbf{x}, t) = -\gamma'S_l^0(\mathbf{x}, t) + i\Omega_c(t)P_l^0(\mathbf{x}, t), \tag{15}$$

where $\mathcal{E}_l^0(\mathbf{x}, t)$ and $P_l^0(\mathbf{x}, t)$ are defined similarly.

We solve the two sets of dynamical equations for $O_l(\mathbf{x}, t)$ and $O_l^0(\mathbf{x}, t)$, respectively, starting from the boundary distributions of the electromagnetic field profiles at the entries to the ensembles. This boundary value treatment circumvents the difficulty in solving the dynamical equations as initial value problems, because the latter should consider the initial photon pulse profiles outside the medium, whose spatial sizes are tremendously larger than those of the slowly propagating ones inside. We apply a fourth-order Runge-Kutta method

in the iterative procedure toward the field profiles $\mathcal{E}_l$, P_l, and S_l. Together with another set of field profiles $\mathcal{E}_l^0$, P_l^0, and S_l^0, we obtain the updated distribution of the effective potential $V_l^{\text{eff}}(\mathbf{x}, t)$ at a specific moment. Compared with the equations for the two-particle functions $OO(\mathbf{x}, \mathbf{x}', t)$ [19], which have nine components, our dynamical equations for the field profiles $O_l(\mathbf{x}, t)$ are much more simplified. For two identical input photon pulses, one only needs to solve the equations for three components of $O_1(\mathbf{x}, t)$ or $O_2(\mathbf{x}, t)$, which are symmetrically distributed with respect to those of the other pulse.

Since we consider the dynamically evolving pulses, the boundary condition for solving the two groups of dynamical equations for $O_l(\mathbf{x}, t)$ and $O_l^0(\mathbf{x}, t)$ should be time dependent as the varying fluxes of photons at the entries of the atomic ensembles. This is in contrast to the time-independent steady state treatment in some previous works. The electromagnetic field of an input pulse is given the profile $\Omega_p(\rho, t) = \Omega_p^M e^{-(t-t_p)^2/\tau_p^2}J_0(2\nu_{01}\rho/d)$ as such a time-dependent boundary condition at the ensemble entries, where Ω_p^M is the maximum of the photons' Rabi frequency $\Omega_p(t) = g\mathcal{E}_l(t)$ that is proportional to the Fourier transform $f(t)$ of the amplitude $f(\omega)$ in Eq. (8), and t_p and τ_p are the timescales indicating the peak arrival and pulse duration, respectively. A single transverse mode $J_0(2\nu_{01}\rho/d)$, the Bessel function of order zero with its first zero point ν_{01}, is considered here without loss of generality.

III. NUMERICAL SIMULATION AND DISCUSSION

A. Storage retrieval of photon pulses

An important feature in the current work is that the control field Ω_c is time dependent, and it takes the form

$$\Omega_c(t) = \Omega_c^M \tanh\{(t_{\text{off}} - t)/\tau_{\text{off}}\}, \quad t \leqslant t_{\text{off}},$$
$$\Omega_c(t) = 0, \quad t_{\text{off}} < t < t_{\text{on}},$$
$$\Omega_c(t) = \Omega_c^M \tanh\{(t_{\text{on}} - t)/\tau_{\text{on}}\}, \quad t \geqslant t_{\text{on}} \tag{16}$$

during a process of stopping and regenerating the photon pulses. Here the field is turned off from its maximum Ω_c^M at the time t_{off} and at the speed determined by τ_{off}. In order to realize the storage of photons, the photon pulses should have a sufficiently long duration τ_p to match the limited width of the EIT window. Such spatially extending photon pulses will be mapped to spinwave packets distributing over the ensembles, after the control field is turned off. A good choice is that the input photon pulses and the control field should be resonantly coupled to the energy levels so that a larger EIT window will be available to avoid high absorption. Certainly one can take a stronger control field to widen the EIT window, but this practice suppresses the induced spinwave, as seen from the relation $S_l(\omega_p) = g\sqrt{N}\mathcal{E}_l(\omega_p)/\Omega_c$ when the concerned interaction is negligible. Figure 2 illustrates the examples of the storage-retrieval processes of copropagating and counterpropagating pulses with $\Delta_p = \Delta_c = 0$ (resonantly coupled to the energy levels) and $\tau_p = 7.0$ μs. As shown in Fig. 2, copropagating pulses are absorbed more significantly than the counterpropagating ones, because the interaction time for the former is much longer. The interactions between counterpropagating
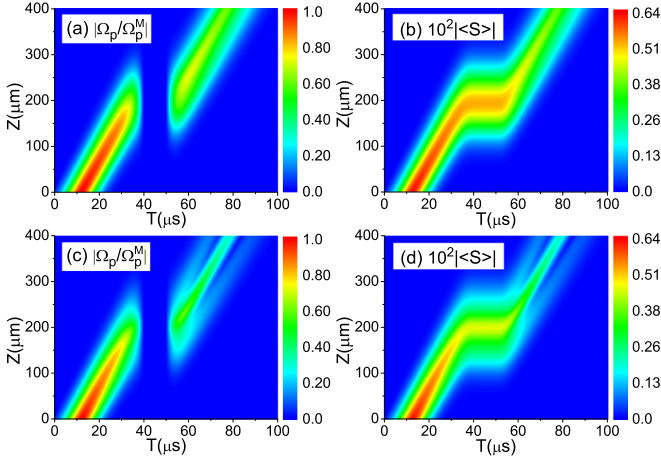
FIG. 2. Dynamical evolutions of photon pulses (a) and (c) and the induced spinwave in the unit $\mu m^{-3/2}$ (b) and (d) throughout a whole storage-retrieval process. Two pulses counterpropagate in (a) and (b) and copropagate in (c) and (d). Two 400-μm-long ensembles fill with ^{87}Rb atoms of the level scheme $|g\rangle = 5S_{1/2}$, $|e\rangle = 5P_{3/2}$, and $|r\rangle = 100S_{1/2}$, with $C_6 = -2.3 \times 10^5$ GHz μm^6, $\gamma = 2\pi \cdot 6.1$ MHz, and $\gamma' = 1.8$ kHz. The control field switch off (on) at $t_{off} = 40$ μs ($t_{on} = 50$ μs) with $\tau_{off} = \tau_{on} = 5$ μs and $\Omega_c^M = 2\pi \cdot 2$ MHz. The parameters of the photon pulses are $\Omega_p^M = 0.01$ MHz, $t_p = 12.0$ μs, and $\tau_p = 7.0$ μs, and those of the ensembles are $N = 2 \times 10^{13}$ cm^{-3}, $a = 10$ μm, and $d = 2$ μm.

pulses increase slowly and become compatible to those of copropagating pulses only when they get close to each other. After the pulses are completely stopped, their losses only come from the slow decay of the Rydberg levels. These results indicate that counterpropagating pulses can better survive in a storage-retrieval process than the copropagating ones.

B. From propagating photon pulses to stationary spinwave packets

The distance between two ensembles is relevant to the spatial distribution of the stopped spinwave packets and their corresponding interaction potential. For two counterpropagating pulses, the absorption of their fronts due to stronger interaction gives rise to deformed spinwave packets; see Fig. 3(a1). The obtained stationary spinwave packets exert an interaction potential V_l^{eff} in Eq. (12) on the other ensembles. Generally this potential is longitudinally inhomogeneous as in Figs. 3(b1) and 3(b2). A nearly homogeneous interaction potential is realized with the largest a in Fig. 3(b2). Applied to photon-photon gate operations, an ideal gate performance requires that each point on a stored wave packet be under a potential of the same magnitude to gain a uniform conditional phase. Therefore a trade-off between the intensity and the uniformity of the achieved Rydberg spinwave interaction exists. Approximately homogeneous potentials like the one in Fig. 3(b2) can be realized with larger ensemble separations. In this regime beyond certain ensemble separation, the difference of the interaction potential distributions from the copropagation and the counterpropagation of the pulses is insignificant. The spinwave profiles of the stopped pulses depend on the τ_{off} as shown in Figs. 3(c1) and (c2). The pulses will be stopped after turning off the control field, to have them immediately stopped by a fast switching with small τ_{off}. One question is whether the nonadiabatic correction accompanying the fast switch will lead to considerable pulse loss as in an ordinary EIT medium [38]. This speculation can be clarified by our numerical calculations that go beyond the adiabatic passages previously studied as in, e.g., Ref. [39]. Our simulations shown in Figs. 3(c1) and 3(c2) demonstrate an unremarkable difference between the disparate switching speeds.
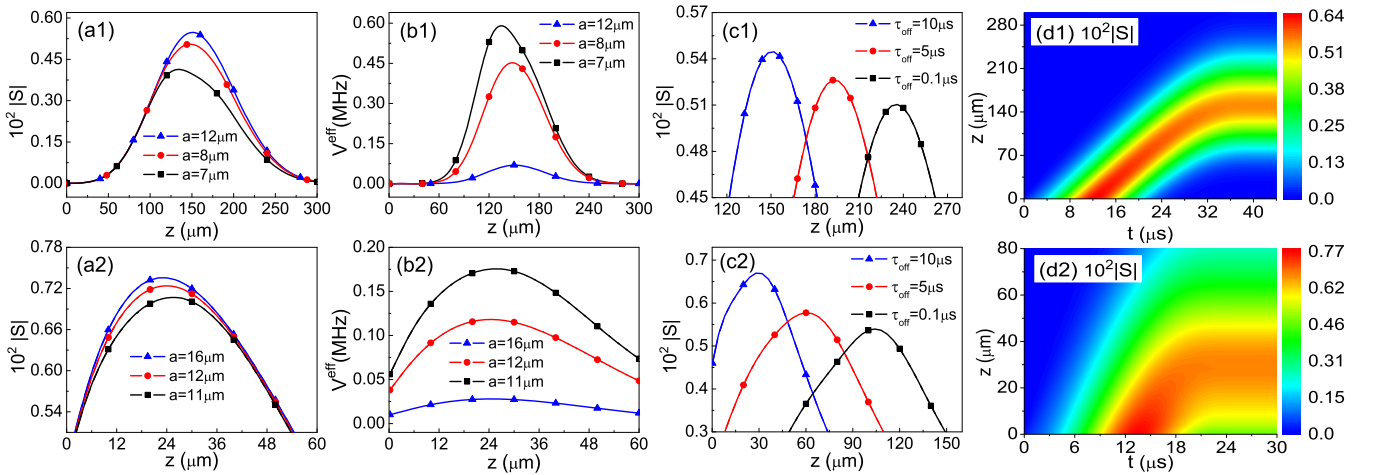
FIG. 3. (a1)–(d1) Two pulses counterpropagating are stopped in two 300-μm-long ensembles given a control field being switched off with $\tau_c = 10$ μs, $t_{off} = 40$ μs. (a2)–(d2) The corresponding quantities for the copropagating pulses, while the control field is turned off at $t_{off} = 24\mu$s. Ensemble length for copropagation is flexible as long as the together pulses can be contained inside. (a1) and (a2) Spinwave profiles and (b1) and (b2) corresponding potentials $|V^{\text{eff}}(z)|$ as functions of a (the distance between the two ensembles). Spinwave profiles obtained from stopping counterpropagating pulses (c1) and copropagating setup (c2) at different switch speeds ($a = 10$ μm). Example of counterpropagating spinwave dynamics [(d1) $a = 10$ μm] and copropagating spinwave dynamics (d2). Here $\Omega_c^M = 2\pi \cdot 2$ MHz and other parameters are the same as those in Fig. 2.
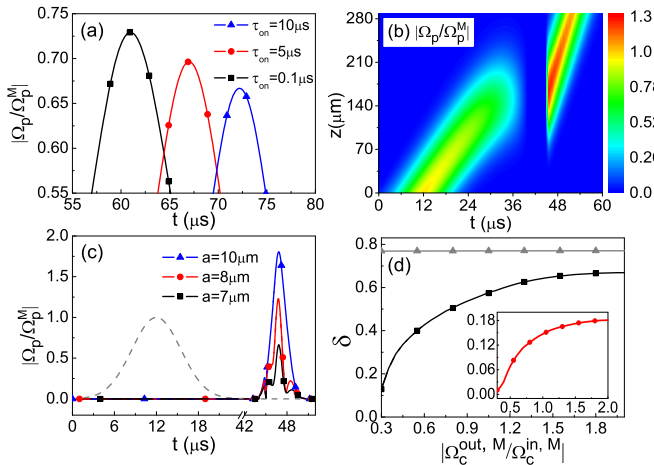
FIG. 4. (a) Ratios of the Rabi frequency of a regenerated photon (at the exit) over the peak value of the input photon's Rabi frequency, given $\Omega_c^{\text{out},M} = 2\pi \cdot 2$ MHz and $a = 10\,\mu$m. (b) Example of photon pulse evolution throughout a whole "write-in" and "read-out" process, for which we chose $\Omega_c^{\text{out},M} = 2\pi \cdot 3$ MHz, $\tau_c = 0.1\,\mu$s, and $a = 10\,\mu$m. (c) Profiles of the photon pulses upon regeneration, given $\Omega_c^{\text{out},M} = 2\pi \cdot 5$ MHz and $\tau_c = 0.1\,\mu$s. The dashed curve is the profile of the input photons for comparison. (d) Growth of the photon survival probability with the ratio of maximum read-out over maximum write-in Rabi frequency, with $\tau_c = 0.1\,\mu$s and $a = 10\,\mu$m. The horizontal line is the corresponding probability achieved without the interaction between pulses. The inset shows the tendency for $a = 8\,\mu$m. The stopping of photons ahead of the regenerating processes here, except for those of $a \neq 10\,\mu$m, is the same as the one in Fig. 3(d1) with $\Omega_c^{\text{in},M} = 2\pi \cdot 2$ MHz and $\tau_{\text{off}} = 10\,\mu$s.

C. Optimal strategy of retrieving photons

The fact that the dissipation due to a fast switch of control field is not significant compared with the losses from other factors helps to determine the optimal way of regenerating photons. Given the retrieval control fields as those in Fig. 1(b), a quick retrieval with small τ_{off}, which lets the retrieved pulses interact for less time, outdoes a slow one as shown in Fig. 4(a). It means that the loss due to the interaction during retrieval is much higher than that from a nonadiabatic process. More improvement can be achieved by retrieving the pulses with a stronger "read-out" control field $\Omega_c^{\text{out}}(t)$. Figure 4(b) illustrates an example of enhancing the retrieved field component $\int dz |\mathcal{E}_l(z)|^2$ in the medium with a stronger $\Omega_c^{\text{out}}(t)$, so that the correspondingly reduced spinwave constituent lowers the interaction between pulses and the associated dissipation. Heavy losses, however, still exist for the regenerated pulses under stronger interaction as seen from Fig. 4(c), where only a small portion of photon pulses compared with the input ones can be regained with the ensembles separated by a shorter distance.

As we learn from Fig. 2, the storage-retrieval efficiency for counterpropagating pulses is better than that of the co-propagating pulses. Here we investigate the optimal way for retrieving stored photons simply by considering the counter-propagating pulses. A proper figure of merit, which measures how well a pulse could survive a whole storage and retrieval process, is the ratio $\delta = \int dt |\mathcal{E}_l(z_{\text{out}}, t)|^2 / \int dt |\mathcal{E}_l(z_{\text{in}}, t)|^2$ of the photon flux at the exit z_{out} and the entry z_{in}, respectively. It approaches a unit value given no photon loss. The realistic photon losses from other factors (such as a limited EIT width) without pulse interaction lead to a ratio δ being less than unit and almost independent of $\Omega_c^{\text{out}}(t)$ [see Fig. 4(d)]. From the example in Fig. 4(d), the loss due to the interaction during retrieval is seen to be reduced by a strengthened "read-out" field, saturating to the ratio δ as it would be completely eliminated by a very fast process to separate the regenerated pulses. The gap between the saturated ratio δ by a large $\Omega_c^{\text{out}}(t)$ and that of a corresponding storage-retrieval process under no interaction is due to the interaction induced loss during stopping photons.

IV. CONCLUSION

We have presented the details of stopping and regenerating individual photon pulses under their mutual interaction in a high density cold Rydberg atomic ensemble. Such processes of single-photon pairs are rather different from those of multiphoton pulses that can be described by the SA model. We adopt a fully dynamical simulation based on first principles to study the processes. An important finding is that, in contrast to the storage-retrieval processes in an ordinary EIT medium, the photon loss due to nonadiabatic effect is insignificant as compared with those from pulse interaction and limited EIT window, so it is flexible to choose a control field for stopping and regenerating photons. Our dynamical approach demonstrates how the storage-retrieval efficiency can be controlled by adjusting the distance between photon pulses and the switch speed of a control field. The optimal way of retrieving the stored photons with a fast switch-on of stronger read-out field is illustrated. The results can provide deeper understanding of some previously proposed quantum information processing setups [22,23]. The approach we apply is generalizable to the processes involving a larger number of photon pulses, which are meaningful to the realistic quantum information processing based on Rydberg media.

[1] J. D. Pritchard, K. J. Weatherill, and C. S. Adams, in *Annual Review of Cold Atoms and Molecules*, edited by M. Kirk *et al.* (World Scientific, Singapore, 2013), Vol. 1, pp. 301–350.

[2] D. E. Chang, V. Vuletić, and M. D. Lukin, Nat. Photon. **8**, 685 (2014).

[3] O. Firstenberg, C. S. Adams, and S. Hofferberth, J. Phys. B **49**, 152003 (2016).

[4] C. Noh and D. G. Angelakis, Rep. Prog. Phys. **80**, 016401 (2017).

[5] I. Friedler, D. Petrosyan, M. Fleischhauer, and G. Kurizki, Phys. Rev. A **72**, 043803 (2005).

[6] B. He, A. V. Sharypov, J. Sheng, C. Simon, and M. Xiao, Phys. Rev. Lett. **112**, 133606 (2014).

[7] J.-H. Wu, M. Artoni, and G. C. La Rocca, Phys. Rev. A **92**, 063805 (2015).

[8] Y. O. Dudin and A. Kuzmich, Science **336**, 887 (2012).

[9] L. Li, Y. O. Dudin, and A. Kuzmich, Nature (London) **498**, 466 (2013).

[10] S. Baur, D. Tiarks, G. Rempe, and S. Dürr, Phys. Rev. Lett. **112**, 073901 (2014).

[11] H. Gorniaczyk, C. Tresp, J. Schmidt, H. Fedder, and S. Hofferberth, Phys. Rev. Lett. **113**, 053601 (2014).

[12] D. Tiarks, S. Baur, K. Schneider, S. Dürr, and G. Rempe, Phys. Rev. Lett. **113**, 053602 (2014).

[13] W. Li and I. Lesanovsky, Phys. Rev. A **92**, 043828 (2015).

[14] C. Tresp, C. Zimmer, I. Mirgorodskiy, H. Gorniaczyk, A. Paris-Mandoki, and S. Hofferberth, Phys. Rev. Lett. **117**, 223001 (2016).

[15] J. Qian and W. Zhang, Phys. Rev. A **90**, 033406 (2014).

[16] E. Distante, A. Padrón-Brito, M. Cristiani, D. Paredes-Barato, and H. de Riedmatten, Phys. Rev. Lett. **117**, 113001 (2016).

[17] Y.-M. Liu, X.-D. Tian, X. Wang, D. Yan, and J.-H. Wu, Opt. Lett. **41**, 408 (2016).

[18] Z. Bai, W. Li, and G. Huang, Optica **6**, 309 (2019).

[19] T. Peyronel, O. Firstenberg, Q. Liang, S. Hofferberth, A. V. Gorshkov, T. Pohl, and M. D. Lukin, and V. Vuletić, Nature (London) **488**, 57 (2012).

[20] O. Firstenberg, T. Peyronel, Q. Liang, A. V. Gorshkov, M. D. Lukin, and V. Vuletić, Nature (London) **502**, 71 (2013).

[21] B. He, A. MacRae, Y. Han, A. I. Lvovsky, and C. Simon, Phys. Rev. A **83**, 022312 (2011).

[22] D. Paredes-Barato and C. S. Adams, Phys. Rev. Lett. **112**, 040501 (2014).

[23] M. Khazali, K. Heshami, and C. Simon, Phys. Rev. A **91**, 030301(R) (2015).

[24] B. He, Q. Lin, and C. Simon, Phys. Rev. A **83**, 053826 (2011).

[25] B. He and A. Scherer, Phys. Rev. A **85**, 033814 (2012).

[26] D. Tiarks, S. Schmidt, G. Rempe, and S. Dürr, Sci. Adv. **2**, e1600036 (2016).

[27] K. M. Beck, M. Hosseini, Y. Duan, and V. Vuletić, Proc. Natl. Acad. Sci. USA **113**, 9740 (2016).

[28] Z.-Y. Liu, Y.-H. Chen, Y.-C. Chen, H.-Y. Lo, P.-J. Tsai, I. A. Yu, Y.-C. Chen, and Y.-F. Chen, Phys. Rev. Lett. **117**, 203601 (2016).

[29] D. Maxwell, D. J. Szwer, D. Paredes-Barato, H. Busche, J. D. Pritchard, A. Gauguet, K. J. Weatherill, M. P. A. Jones, and C. S. Adams, Phys. Rev. Lett. **110**, 103001 (2013).

[30] I. Mirgorodskiy, F. Christaller, C. Braun, A. Paris-Mandoki, C. Tresp, and S. Hofferberth, Phys. Rev. A **96**, 011402(R) (2017).

[31] F. Ripka, Y.-H. Chen, R. Löw, and T. Pfau, Phys. Rev. A **93**, 053429 (2016).

[32] X.-D. Tian, Y.-M. Liu, Q.-Q. Bao, J.-H. Wu, M. Artoni, and G. C. La Rocca, Phys. Rev. A **97**, 043811 (2018).

[33] D. Petrosyan, J. Otterbach, and M. Fleischhauer, Phys. Rev. Lett. **107**, 213601 (2011).

[34] J. D. Pritchard, D. Maxwell, A. Gauguet, K. J. Weatherill, M. P. A. Jones, and C. S. Adams, Phys. Rev. Lett. **105**, 193603 (2010).

[35] P. W. Milloni, *Fast Light, Slow Light and Left-Handed Light* (IOP, Bristol, 2005).

[36] B. He, S.-B. Yan, J. Wang, and M. Xiao, Phys. Rev. A **91**, 053832 (2015).

[37] L. Yang, B. He, J.-H. Wu, Z.-Y. Zhang, and M. Xiao, Optica **3**, 1095 (2016).

[38] M. Fleischhauer and M. D. Lukin, Phys. Rev. A **65**, 022314 (2002).

[39] D. Yan, C.-L. Cui, M. Zhang, and J.-H. Wu, Phys. Rev. A **84**, 043405 (2011).